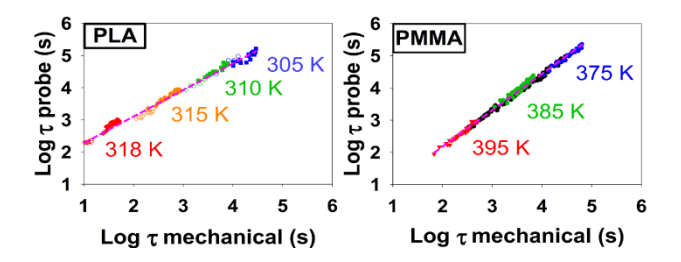
Linear Stress Relaxation and Probe Reorientation – Comparison of the Segmental Dynamics of Two Glassy Polymers During Physical Aging

Josh Ricci*, Trevor Bennin, Enran Xing, and M.D. Ediger

Department of Chemistry, University of Wisconsin - Madison, Madison, Wisconsin 53706, United States *Corresponding Author - Email: jricci@chem.wisc.edu



(For Table of Contents use only)

Abstract

Segmental dynamics of glassy poly(methyl methacrylate) (PMMA) and poly(lactic acid) (PLA) have been measured over 8 hours of aging via both optical probe reorientation and mechanical stress relaxation experiments performed in the linear response regime, in a temperature range between 6 and 30 K below the glass transition temperature (Tg). A clear power law relationship between relaxation times and aging times is observed in all experiments. For both PLA and PMMA glasses, the probe reorientation times are strongly correlated with stress relaxation times over the observed range of aging times and aging temperatures, with the two relaxation times related by a power law with an exponent

of ~1. Comparisons of these data sets with previously published work indicates that the relationship between the two relaxation times is not influenced by secondary relaxation processes, low levels of crosslinking, or the presence of a plasticizer. These results support the view that the probe reorientation technique is a good reporter of segmental dynamics in the glassy state.

Introduction

The ease with which polymer glasses can be produced and shaped coupled with their optical clarity and low density make them ideal materials for an extensive variety of purposes, ranging from aeronautics and medical technologies to textiles and food preparation. The mechanical properties of polymer glasses are often a critical consideration for applications. In the glassy state, polymers exhibit many behaviors that are incompletely understood, such as a transition from brittle to ductile behavior at a given temperature, ¹⁻² or a temporal evolution of material properties in response to mechanical deformation. ³⁻⁶ A full description of the mechanical response of glassy polymers remains elusive.

In the glassy state, an important material characteristic of a polymer is the segmental relaxation time, τ , which describes the time required for a few segments of the polymer chain to rearrange into a new configuration. In the glass, τ may be on the order of hours or days. If a small perturbation is applied and quickly released, the glass will respond as an elastic solid. On the other hand, if a larger force is applied and maintained, the material response will be non-linear, giving rise to a number of well-known glassy behaviors, such as yielding, and strain softening, leading eventually to a plastic flow regime, where the material behavior qualitatively resembles that of a viscous liquid. This change from solid-like to liquid-like behavior reflects an underlying decrease in τ as the experiment proceeds. A reduction in τ as a result of non-linear deformation has been a feature of theories of polymer deformation dating back to Eyring.⁷ Over the last 15 years, deformation-induced changes in τ have frequently been observed in simulations, $^{8-10}$ and are a key aspect of virtually all modern theoretical

approaches to polymer glass deformation. Understanding the evolution of τ during non-linear deformation is key to understanding yielding and plastic flow and a quantitative description of this behavior is an open research question.

Experiments are playing a key role in understanding how the segmental relaxation time τ in a polymer glass evolves during deformation. Dielectric experiments are easily capable of direct measurements of τ at high temperatures (above the glass transition temperature, T_g), where τ is short. While such experiments have been performed on polymer glasses during deformation, t^{17-18} the range of temperatures for which τ can be observed is limited. Mechanical experiments, such as creep and stress relaxation measurements, are common tools for the determination of τ in the glassy state, allowing for a straightforward measurement that can be performed on any polymer glass. Such mechanical tests allow for easy comparison between results from many different polymers, but mechanical tests provide direct access to τ only in the linear response regime. Such mechanical tests provide direct access to τ only in the linear response regime. The past decade, Ediger and coworkers have developed an alternate strategy for monitoring τ during active non-linear deformation of a polymeric glass. The reorientation of probe molecules embedded in the polymer matrix can be used to access segmental dynamics even while the sample is being deformed, and this technique is capable of measuring relaxation times larger than those so far accessible by dielectric methods. Results from this method have been used to test theoretical approaches that describe polymer deformation. Such as the polymer deformation of the polymer deformation.

While the probe reorientation technique provides a window into polymer dynamics during non-linear deformation, as the detection of mobility occurs indirectly through a probe, control experiments are needed to establish the accuracy of the method. In the polymer melt state above T_g, probe reorientation measurements show a similar temperature dependence as dielectric and mechanical relaxation measurements.^{4, 22, 29-30} Recently a test has been performed at temperatures below T_g on lightly crosslinked PMMA, comparing the probe reorientation technique with stress relaxation

measurements in the limit of a linear deformation.³¹ The probe reorientation time was found to be strongly correlated with the stress relaxation time and related by a power law exponent near 1.0. These efforts collectively establish that the probe reorientation time is an accurate reporter of mobility for crosslinked PMMA, both in and out of the glassy state, in the limit of linear deformations. While this lends support to the notion that probe reorientation results collected under active non-linear deformation (a regime where comparisons with other techniques are largely unavailable) accurately represent the dynamical changes occurring in the sample, crosslinked PMMA is only one polymer system and does not represent the full scope of polymeric behavior.

Here we compare two techniques, probe reorientation and linear stress relaxation, as methods to interrogate segmental relaxation times of two aging polymer glasses, poly(lactic acid) (PLA) and uncrosslinked PMMA. PMMA is a widely used engineering polymer that is readily vitrified into an amorphous state. PMMA is frequently used as a prototypical glassy polymer, and has been extensively researched and characterized, 1, 14, 21, 31-38 providing a large set of data against which our results may be compared. The results on uncrosslinked PMMA in the experiments presented here also allows for a comparison against data previously collected from lightly crosslinked PMMA,³¹ in order to evaluate the effects of low levels of crosslinking upon the dynamics and aging behavior. In contrast, PLA forms a biodegradable plastic, and has been the focus of much recent research aimed at developing a more sustainable option in plastic manufacture. ³⁹⁻⁴³ As an additional consideration, PLA has properties that differ from PMMA in several important ways. PMMA displays a very broad distribution of relaxation times, which may lead to a systematic error in experimental measurements confined to a narrow measurement window. In contrast, the distribution is substantially narrower in PLA.⁴⁴ PMMA is also known to exhibit a secondary relaxation that, at temperatures near to Tg, can overlap with the main relaxation process. 45-46 By comparing results against PLA, which exhibits no such overlapping processes in the temperature range evaluated here, 44,47 we can evaluate the effect of a secondary process on

aging as detected by the two experimental techniques. Finally, PLA is a hygroscopic material, and becomes plasticized with increasing water content, directly altering the relaxation dynamics at a constant temperature.⁴⁸ This allows an examination of the effects of plasticization on the relaxation times as measured by the two techniques.

For glasses of both PMMA and PLA, we find that the probe reorientation times and the stress relaxation times show a strong correlation over a range of aging times (t_a) and aging temperatures. The two types of relaxation times have a power law relationship with an exponent near 1. Comparisons of data for these two polymer glasses, and comparisons with previously published work on crosslinked PMMA, indicate that the relationship between the two relaxation times is not influenced by secondary relaxation processes, low levels of crosslinking, or the presence of a plasticizer. These results support the view that the probe reorientation technique is a good reporter of segmental dynamics in the glassy state.

Methods/Materials

Polymer samples were prepared via solvent casting. Poly (methyl methacrylate) (PMMA, $M_w = 1,544,000 \, \text{g/mol}$) was purchased from Scientific Polymer Products. Poly (lactic acid) (PLA, $M_n \approx 150,000 \, \text{g/mol}$, 50/50 D/L ratio) was purchased from PolySciTech. Both were employed without additional purification. Quantities of the polymer materials were dissolved into dichloromethane, and the optical probe N,N'-dipentyl-3,4,9,10-perylenedicarboximide (DPPC, Aldrich, 76372-75-3) was added such that the final probe concentration was $^{\sim}10^{-6} \, \text{M}$ with respect to the solid polymer, small enough that any plasticization effects are negligible. The mixture was poured into flat bottomed glass petri dishes, and covered with ventilated aluminum foil to control the rate of evaporation. Rapid evaporation of the solvent tended to produce films of uneven thicknesses. After drying for 24 hours, t films were then placed under vacuum, and held at an elevated temperature (343 K for PLA, 393 K for PMMA) for 24

hours to remove the remaining solvent. Film thicknesses following this process were between 25 and 40 micron. Dog bone samples were cut from the films using a custom steel dye. The samples so produced correspond to ASTM D1780-10 in shape, though scaled down in size. The tacticity of the polymers utilized was evaluated via proton NMR experiments. The PMMA chains were 6% isotactic, 74% syndiotactic, and 20% heterotactic. For the PLA sample, NMR results indicate that the material is comprised of a racemic mixture of D-lactide, and L-lactide dimers;⁴⁹ more precise characterization was limited by overlapping spectral features. Based upon preparation conditions, the crosslinked PMMA samples used in our earlier work (data shown here for comparison)³¹ are expected to be 6% isotactic, 60% syndiotactic, and 34% heterotactic.³⁷

DSC measurements give T_g for PMMA as 404.5 +/- 0.75 K, and for PLA as 324.5 +/- 0.5 K as measured from the midpoint of the transition upon heating at 10 K/min, after cooling at 1 K/min for PMMA, or 0.5 K/min for PLA. Repeated annealing of the samples at 412 K for PMMA and 335 K, as performed during our optical and mechanical experiments, caused no change in T_g and no change in mechanical or optical relaxation times. Annealing the samples at considerably higher temperatures that those used in our experiments resulted in slight increases in T_g (\leq 1 K) consistent with the presence of a small amount of solvent, which was confirmed by thermal-gravitational analysis.

Instrumentation/Apparatus

The instrument that allows simultaneous mechanical deformation and probe reorientation measurements has been described in detail elsewhere.^{22,31} In brief, the sample is held in sandpaper-lined grips at each end, and housed within a temperature controlled brass cell that includes a glass window through which optical data can be obtained. One end of the sample is held stationary, while the position of the other is controlled by a linear actuator, which allows for fine control over both the extent of strain, and the rate at which it is applied. The applied force is continually monitored by a 5 N

load cell. The deformation apparatus is stationed atop a confocal microscope to allow for measurement of fluorescence emitted from the probe molecules. The collected fluorescence is divided into two optical channels via a polarizing beam splitter, and the output of each channel is independently measured with an avalanche photodiode.

Thermal protocol

The sample is initially heated to the annealing temperature, 412 K ($T_g + 7.5 \text{ K}$) for PMMA, and 335 K ($T_g + 9.5 \text{ K}$) for PLA, and held for ~30 minutes. The sample is then cooled at a controlled rate (1 K/minute for PMMA and 0.5 K/minute for PLA) to the testing temperature. PLA is cooled more slowly because the annealing temperature is only slightly above room temperature, and the apparatus cannot reach the same cooling rate as in the PMMA experiments. Following cooling, the sample is held isothermally at the testing temperature for the remainder of the experiment. The zero time for physical aging is the point where the sample temperature reaches the calorimetrically-determined T_g . We considered the impact of this particular choice for zero time. Analysis of the DSC results indicates that the fictive temperature of a sample cooled at 1 K/min might be up to 2 K less than the determined T_g value. To determine the impact of this on our results, we shifted our zero time by 4 minutes (which is the largest amount consistent with a 2 K error) and reanalyzed our results. The difference is not consequential for our discussion. For example, the μ values presented in Figure 8 below would shift by at most the size of the data points, and much less than indicated error bars.

Stress Relaxation Experiments

The details of the stress relaxation protocols have been previously reported elsewhere.³¹ Briefly, the sample is subjected to a strain of 0.5%, with an applied strain rate of $\sim 10^{-2}$ /s. The stress is subsequently monitored, with time t=0 taken as the midpoint of the strain step. Stress relaxation

experiments are performed according to a modified Struik protocol that we have previously employed, with data collected at aging times that increase by a factor of 2, and measurement durations limited to 10% of the aging time. This protocol is intended to minimize both the effects of aging that occurs while the stress relaxation is proceeding, as well as the impact of a given measurement on the results of succeeding measurements. We record data points rapidly during the deformation to more accurately determine the deformation time and the peak stress value, and then at a slower rate after the peak stress in order to limit the size of the data files. This switch results in loss of data (for about a second) in the stress relaxation curve immediately following the end of the deformation. For most experiments, the effects of this gap is minimal, with the first recorded data point after the change measuring stresses between 87 and 95% of the observed peak stress. At the highest temperatures measured in the PLA experiments (318 K) however, the effect was larger and the strain rate was increased to $\sim 1.5 \times 10^{-2}$ in order to minimize relaxation during the imposition of the strain.

Probe Reorientation Experiments

Full details of the probe reorientation technique have been published previously. ²²⁻²³ Before the measurement begins, the probe molecules are oriented isotropically. The reorientation experiment is initiated by exposing the sample to a linearly polarized laser. Probe molecules with transition dipoles oriented near to the laser polarization will be more likely to be photobleached, resulting in an anisotropic orientational distribution for the unbleached molecules. A circularly polarized reading beam is then used to induce fluorescence. The fluorescence is passed through a polarizing beam splitter, dividing the emitted light into components polarized either parallel or perpendicular to the polarization of the bleaching beam. Immediately after the bleach, these two optical channels will display very different intensities, but as time proceeds the unbleached probes will gradually return to an isotropic distribution, eliminating the observed difference in fluorescence intensities. The intensity values can be

used to calculate an anisotropy function, R(t), whose decay describes the reorientation of the probe molecules. The decay of the anisotropy over time can be fit to a stretched exponential function (see below), yielding a characteristic probe reorientation time τ . The sample is held at a low level of stress (~0.3 MPa) for the duration of the optical experiment to prevent sample movement; this stress is not sufficient to affect the measured relaxation times. To minimize the influence of noise, the probe reorientation measurements are collected over a longer timescale than the stress relaxation measurements. The measurement time for optical experiments varies with temperature and aging time, but exceeds 50% of the aging time at the onset of the experiment in only ~5% of measurements.

KWW Fitting

Stress relaxation and anisotropy decay curves are fit using the same functional form, the KWW or stretched exponential function:

$$R(t) \ or \ \sigma \ (t) = A \ exp^{-(\frac{t}{\tau})^{\beta}} \tag{1}$$

where A reflects the value of anisotropy (or stress) at time t=0. τ indicates a characteristic relaxation time which corresponds to the time required for the observable (anisotropy or stress) to decay from its initial value by a factor of 1/e. The stretching exponent, β , is taken as an indicator of the width of the distribution of relaxation times. Differing definitions of the relaxation time can be found in the literature, but in this work τ exclusively refers to times extracted from equation (1).

For the stress relaxation measurements, the value for β is determined by generating a time-aging time master curve for each 8 hour aging experiment. When fitting an individual stress relaxation curve, the β value is constrained to the value obtained from an unconstrained fit to the associated time-aging time master curve. For PLA, the values of β obtained from different time-aging time master curves were very similar, near 0.41, independent of aging temperature. For PMMA, at each aging temperature, the

values of β obtained from different experiments were very similar but the average value of β did show a small temperature dependence, varying from 0.29 at 375 K up to 0.37 at 395 K. As discussed below, results from the stress relaxation experiments, as well as the success of time-aging time and time-temperature superposition for all data sets, support the view that β remains approximately constant across all experimental conditions. β values obtained from unconstrained fits to individual stress relaxation curves are presented in the Supplemental Information; these fits are not utilized in our data analysis.

Because of the greater noise present in the optical measurements, we have elected to constrain β to a constant value in KWW fits. For probe reorientation measurements, this value is determined from long anisotropy decay curves collected from samples that have been aged to equilibrium just below Tg. For probe reorientation measurements on PMMA, β is constrained to 0.31, while in PLA, it is held at 0.50.

In order to assess the impact that the assumption of a constant β may have in our findings, we include in the Supplemental Information comparative figures constructed using the shift factors obtained from superposition of the decay curves; for this procedure, nothing is assumed about the β parameter being constant. As discussed below, our major conclusions are supported by the alternate data analysis scheme.

Results

Anisotropy decay and stress relaxation measurements (PLA)

Probe reorientation and stress relaxation measurements were collected from PLA glasses over a temperature range between 305 K (T_g – 19.5 K) and 318 K (T_g – 6.5 K), and for aging times up to 8 hours. Representative results of these experiments can be seen in Figures 1 (optical) and 2 (mechanical). With

horizontal and slight vertical shifts, data from individual experiments can be collapsed onto a single time-aging time master curve as illustrated for anisotropy decay curves in Figure 1 (upper panels). These isothermal master curves can then be collapsed by the same procedure to form a single unified master curve that accounts for the effects of both temperature and aging time (Figure 1, main). For clarity, data points in the upper panels of Figure 1 are only shown for the master curves. The curves representing individual experiments are KWW fits through the data, with β constrained to the value obtained from an unconstrained KWW fit through the corresponding master curve at each temperature. (These fits were generated to represent the individual experiments; they play no role in the analysis of the data.) The successful superposition of the data for both temperature and aging time indicates that β is approximately constant over all temperatures and aging times examined here. The β value obtained from the fit to the full master curve, shown in the main panel of figure 1, is 0.50. This is consistent with the value of 0.50 obtained from equilibrium measurements at temperatures just below T_8 , and supports the constraint of β to 0.50 for all anisotropy decay curves obtained from PLA in this work.

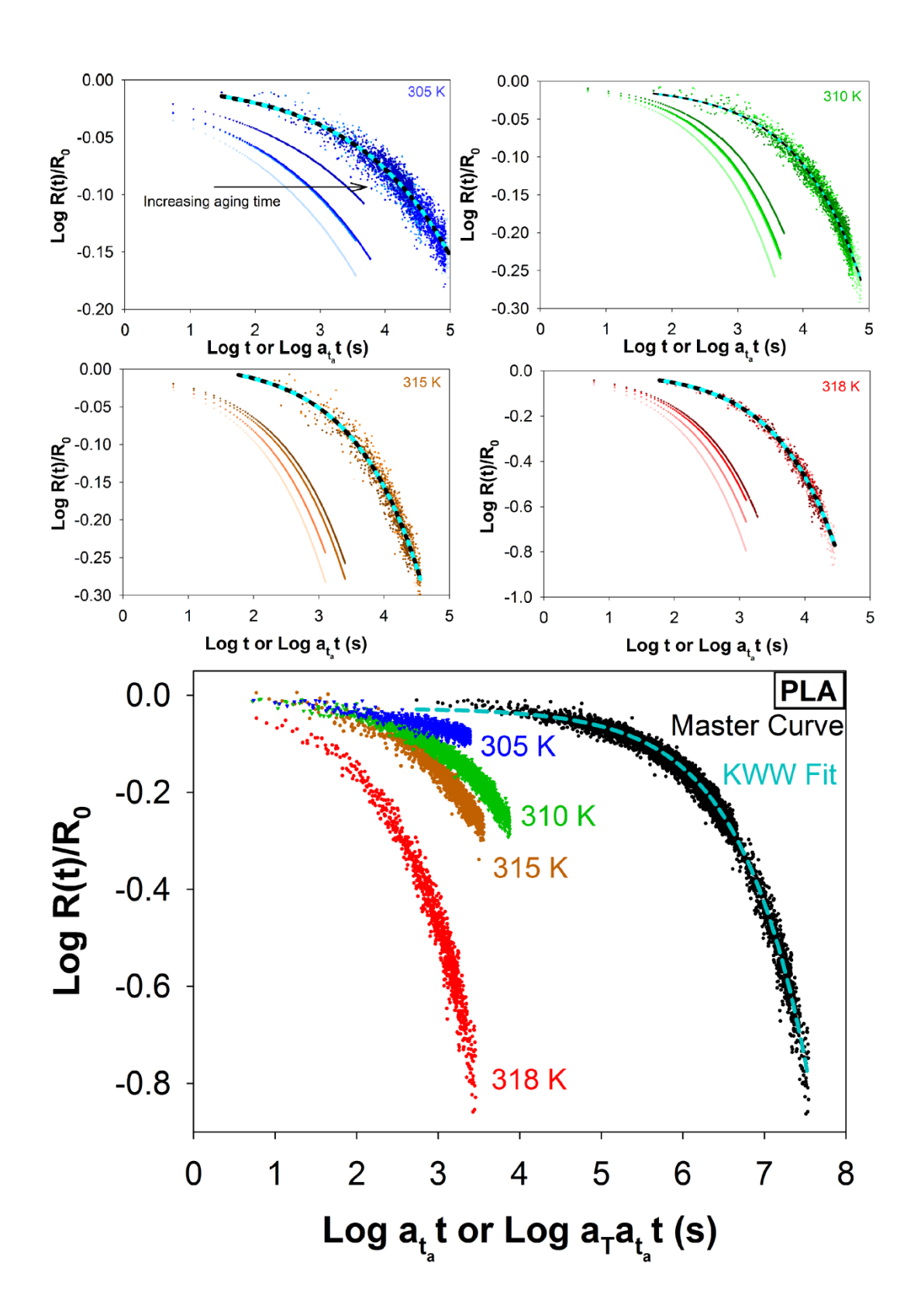


Figure 1. Superposition of anisotropy decay curves from PLA. Upper panels illustrate time-aging time superposition for representative isothermal experiments, with the master curves referenced to the longest aging time. Curves shown are

KWW fits to the data, with β constrained to the value obtained from an unconstrained fit to the associated master curve (dashed black/cyan). Individual data points are shown in the master curve for each temperature but are omitted from the individual measurements for clarity. The main figure illustrates time-temperature superposition of the master curves shown in the upper figures, referenced to the curve at 305 K. The dashed cyan line is an unconstrained KWW fit to the master curve, for which the β value is 0.50. For all plots, the master curves are offset to the right for clarity.

Stress relaxation data also collapses into a single master curve for all aging times and temperatures as shown in Figure 2. The value of β from the fit to the master curve is 0.39, which agrees closely with the average value of 0.42 obtained from unconstrained fits to the superposition master curves generated for each 8 hour experiment. We utilized small vertical shifts when producing the master curves and we assessed the impact of this by also analyzing the data without vertical shifts. The master curve generated without the use of vertical shifts provides the same value of β (within 0.01) as that presented in Figure 2, although the quality of the superposition is clearly degraded with small separations appearing between the isotherms.

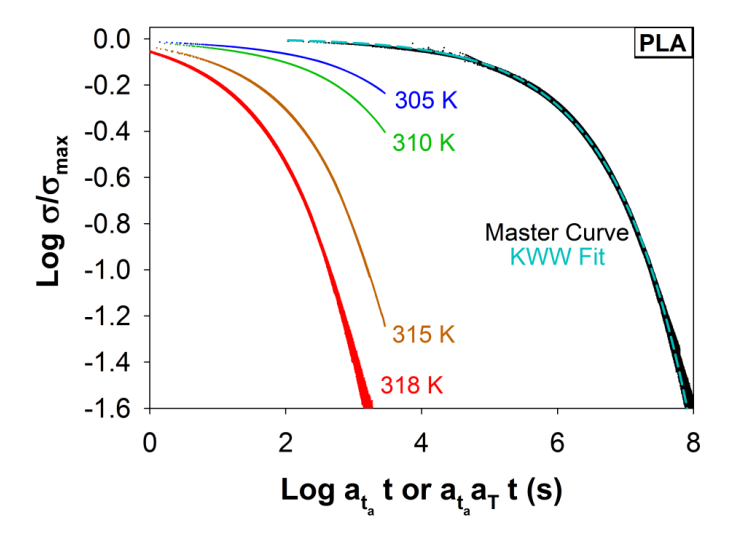


Figure 2. Time-temperature-aging time superposition of all stress relaxation curves (black points, 65 individual experiments) collected from PLA, referenced to data collected at 305 K at 8 hours of aging. An example of an isothermal time-aging time

master curve drawn from an 8-hour aging experiment is shown for each temperature investigated, with temperature indicated by color. The dashed cyan curve is a KWW fit to the master curve, proving a β value of 0.39.

Relaxation times and β values (PLA)

Anisotropy decay and stress relaxation curves were both fit to a KWW function, equation (1), from which values of τ were extracted. For these fits, β values were constrained as described in the Experimental Section. Figure 3 shows τ values as measured at different temperatures and aging times. Relaxation times increase with either increasing aging time, or decreasing temperature. While the effects of temperature upon both the value of τ , and the rate at which τ changes with aging time are strong, we see that measurements from both techniques respond to changes in temperature in similar ways. At any temperature investigated here, the curve describing the probe reorientation time and that describing the stress relaxation time run very nearly parallel to each other. We will return to this point in the discussion section.

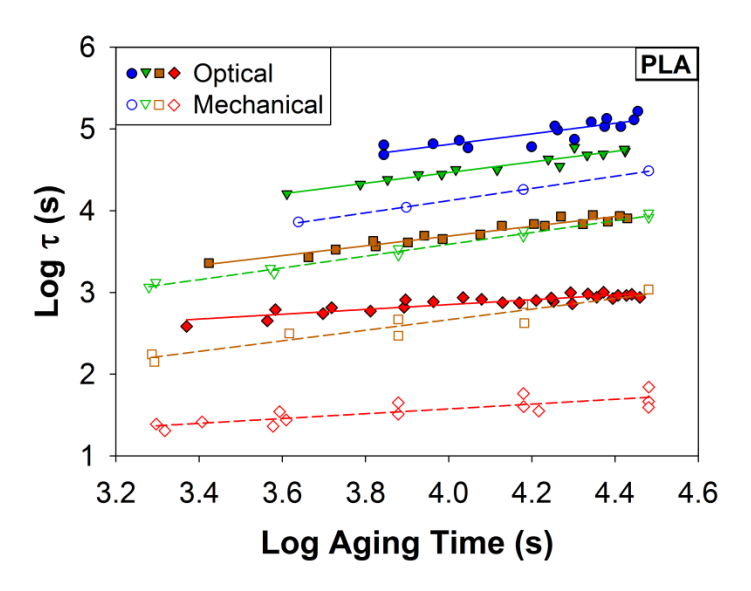


Figure 3. Log relaxation time vs log aging time for PLA experiments performed under low humidity conditions. Solid symbols indicate anisotropy decay measurements, and open symbols indicate stress relaxation measurements. Color indicates

temperature (Red - 318 K, Orange - 315 K, Green - 310 K, Blue - 305 K). Solid and dashed lines indicate linear fits through the optical and mechanical data, respectively.

While the relaxation times shown in Figure 3 were obtained using constrained values of β , we report β values from obtained from unconstrained fitting of individual stress relaxation measurements in the Supplemental Information (Figure S1). Under all conditions tested, we find β values near 0.4. This is consistent with the superposition shown in Figure 2 and supports the view that β is insensitive to changes in temperature and aging time.

Influence of Humidity (PLA)

PLA is known to be hygroscopic, and experiments indicate that water may act as a plasticizer, leading to reductions in T_g and, by extension, relaxation times collected at a given temperature. The data presented in this work was collected over a period of \sim 6 months, during which the relative humidity in the lab shifted with the seasons, ranging from 16% to 62% over the course of data collection. This provided an (unplanned) opportunity to investigate the influence of relative humidity on stress relaxation and probe reorientation times. As shown below, these two measures of segmental dynamics respond identically to changes in relative humidity.

We classify individual experiments as being performed in either high humidity (lab RH > 45%, with an average value of 52%), or low humidity (lab RH < 35%, with an average value of 21%) conditions. We note that the relative humidity in the lab is not the same as the value in the heated deformation cell. We can estimate the relative humidity in the deformation cell by assuming that the partial pressure of water vapor is the same in the lab as in the cell (which allows for easy gas exchange with its

surroundings) and utilizing the Arden Buck equation.⁵¹ The calculated range of the relative humidity in the deformation cell is 4-32%.

Shifts in τ were observed between high humidity and low humidity conditions, consistent with the idea that increasing water content acts to soften the material. An example of such shifts is shown in Figure 4, for both probe reorientation and stress relaxation measurements. The size of the observed shift is consistent between the two techniques, and grows larger as the temperature is increased (not shown). The shifts in τ due to humidity are interpreted as a shift in T_g . As shown in Figure 4, τ differs by ~ 0.35 decades between low and high humidity conditions at 310 K. The difference in τ between measurements at 310 K and 315 K (under either high or low humidity) is ~ 0.75 decades. From this, and similar comparisons at all measured temperatures, we estimate that T_g of the material in high humidity conditions is 2-3 K lower than under low humidity conditions. This is consistent with the experimental findings of Sharp and Forrest, who cite a shift in T_g of ~ 3 K over the range of effective humidities examined here. Only data collected under low humidity conditions has been shown in Figure 3.

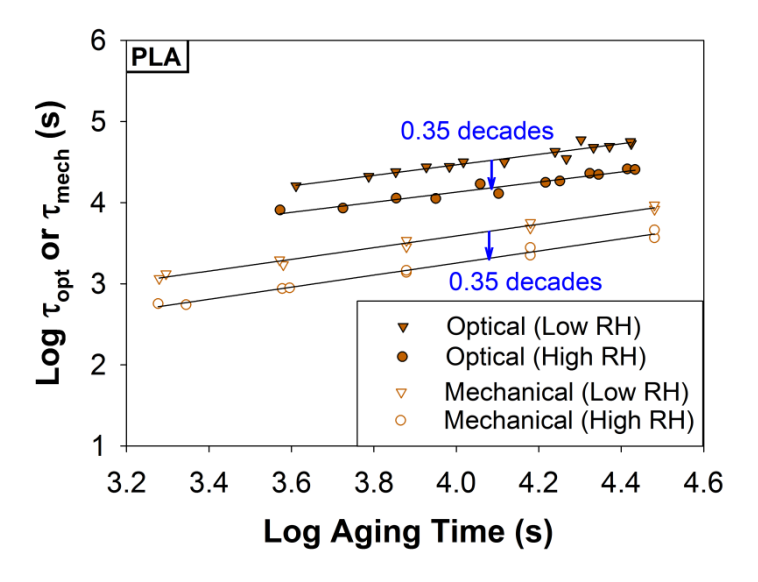


Figure 4. Log relaxation time vs log aging time from probe reorientation and stress relaxation experiments performed at 310 K, and at different levels of relative humidity. Open points indicate mechanical tests, and solid symbols indicate optical

tests. Circles represent data collected under high humidity conditions, and triangles indicate low humidity conditions. Solid black lines are linear fits to the data. The difference between otherwise identical experiments performed under high and low humidity conditions is indicated in blue.

Anisotropy decay and stress relaxation measurements (PMMA)

Probe reorientation and stress relaxation experiments were performed on an uncrosslinked PMMA sample over a range of temperatures from 375 K (T_g – 29.5 K) to 395 K (T_g – 9.5 K). As with the PLA results, data from all temperatures and aging times can be collapsed into a single master curve, indicating that β remains approximately constant over the range of parameters explored in this work. The superposition master plot for all stress relaxation curves collected from PMMA is shown in Figure 5. The individual experiments collapse cleanly into a well-defined curve that can be fit with a KWW function. The KWW fit yields a β value of 0.35. This value agrees closely with the average value of 0.35 obtained from unconstrained fits to superposition master curves generated for each 8 hour experiment, and is just slightly above the value of 0.31 observed in equilibrium probe reorientation measurements. We note that the KWW fit to the PMMA master curve (Figure 5) is not as good as that observed for PLA (Figure 2), with a slight deviation appearing at short times. We will return to this point in the discussion section. As in the case of PLA, the small vertical shifts used in the superposition process did not have a significant impact on the KWW β value determined by this procedure.

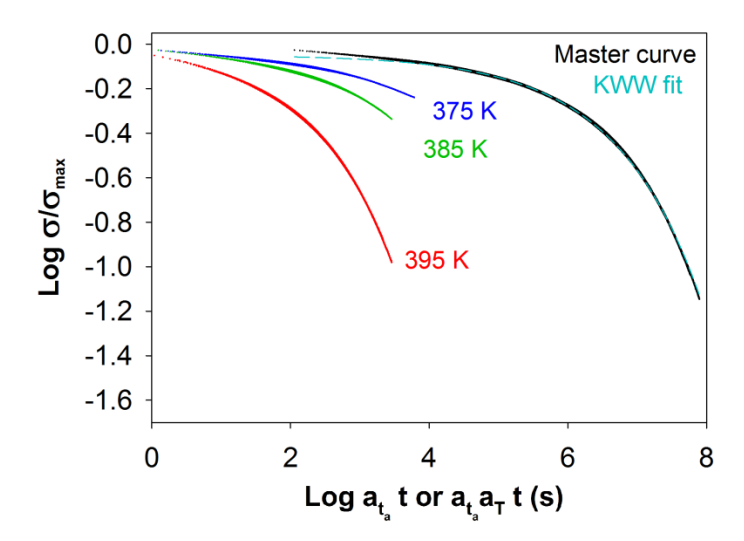


Figure 5. Time-temperature-aging time superposition of all stress relaxation data collected from PMMA (33 individual experiments), referenced to data collected at 375 K at 8 hours of aging. An example of an isothermal time-aging time superposition curve drawn from an 8-hour aging experiment is shown for each temperature investigated, with temperature indicated by color. The master curve (black), and the corresponding KWW fit (cyan) are offset for clarity. The KWW β value for the fit to the master curve is 0.35.

Relaxation times and β values (PMMA)

Relaxation times from probe reorientation and stress relaxation measurements are shown below in Figure 6. For these fits, β values were constrained as described in the Experimental Section. As with PLA, relaxation times increase with increasing aging time and decreasing temperature. Again, we observe that curves from probe reorientation and stress relaxation measurements run very nearly parallel, regardless of the temperature.

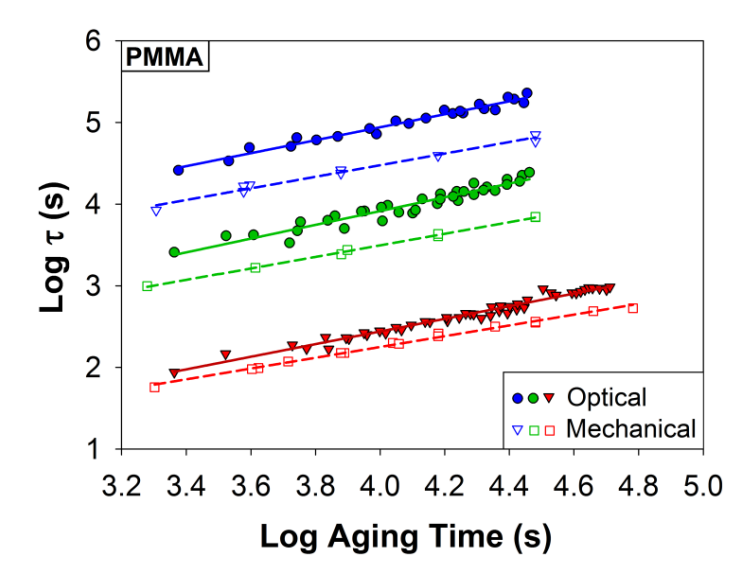


Figure 6. Log relaxation time vs log aging time for PMMA. Solid symbols indicate data collected from probe reorientation experiments, while open points indicate stress relaxation experiments. Temperature is indicated by color (Red - 395 K, Green - 385 K, and Blue - 375 K).

While the relaxation times shown in Figure 6 were obtained using constrained values of β , we report β values from obtained from unconstrained fitting of individual stress relaxation measurements in the Supplemental Information (Figure S2). We observe that β remains to a first approximation unchanged as aging proceeds, however there is a slight but systematic shift with temperature. Such effects have been previously observed in PMMA and other polymers, and are attributed to the observation window not including very short or very long time behavior. From this perspective, it is reasonable that such an effect would be more prominent in PMMA than in PLA, as the former displays a substantially broader distribution of relaxation times. If the observed behavior corresponded to an actual change in the distribution of relaxation times, superpositions of data collected at different temperatures, such as the one shown in Figure 5, should not be possible.

Discussion

Figure 7 shows a direct comparison between probe reorientation and stress relaxation measurements in both PLA (upper) and PMMA (lower). τ values from anisotropy decay curves are determined directly from KWW fits to the raw data, as shown in Figures 3 and 6 (solid points).

Corresponding stress relaxation τ values at the same aging times as for the optical data are interpolated from linear fits to the stress relaxation data shown in Figures 3 and 6 (dashed lines). If the two techniques gave identical values for τ, data in Figure 7 would fall on the line y=x, included as a reference. The lower panel of Figure 7 also includes data for crosslinked PMMA glasses, as published in reference [31]. A strong power law relationship, with an exponent near 1, is observed for both PLA and PMMA, indicating that the two measurements of dynamics are closely related, and are similarly affected by changes in temperature, aging time, and other factors described in more detail below. The behavior of systems examined in this work, especially when compared with the earlier findings from crosslinked PMMA, ³¹ establish that the consistency between probe reorientation and stress relaxation measurements is quite general in spite of the differences among the three polymer glasses studied.

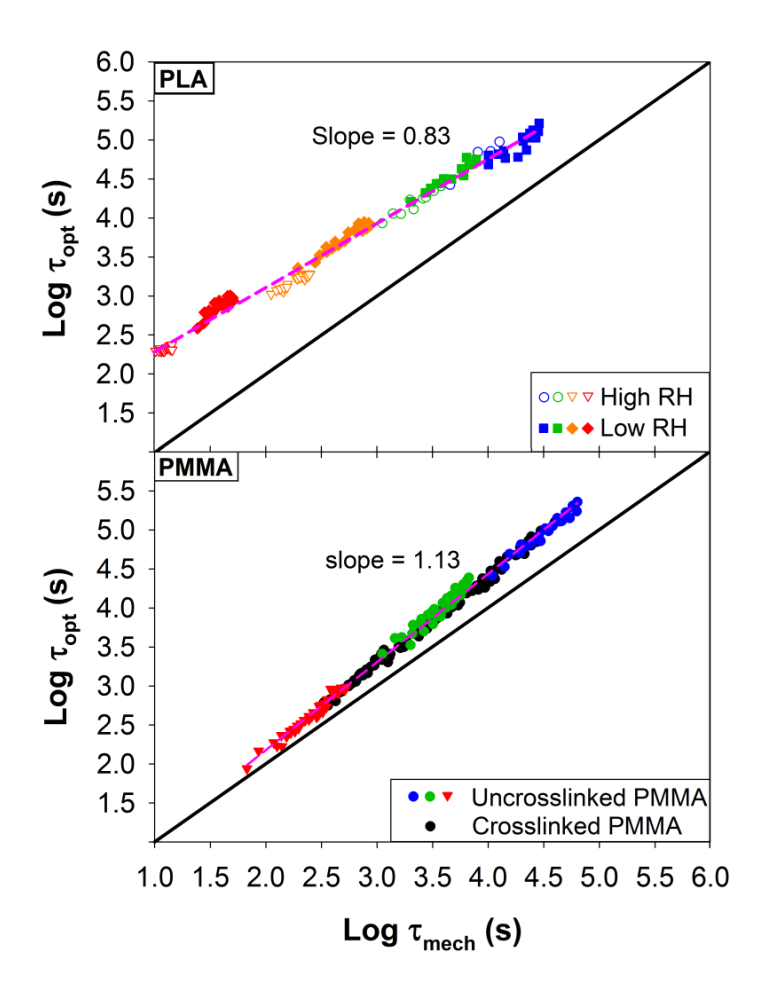


Figure 7. Log-log plot of relaxation times from probe reorientation measurements vs stress relaxation times, constructed from data shown in Figure 3 (PLA), or in Figure 6 (PMMA). Upper (PLA): Color indicates temperature as in Figure 3. Open points indicate data collected under high humidity conditions, solid points indicate data collected under low humidity conditions. Lower (PMMA): Color indicates temperature as in Figure 6. Black points represent data collected in experiments on crosslinked PMMA across a similar range of temperatures, from ref [31].

The effect of humidity upon the segmental dynamics in PLA are demonstrated in the upper panel of Figure 7. The data is separated based on the relative humidity at the time of the experiment. Data collected under high humidity conditions, shown as open points, fall on the same line as data collected under low humidity conditions. This indicates that the plasticization due to increased water content in

the sample equally affects relaxation times from both probe reorientation and stress relaxation measurements.

The effects of low levels of crosslinking are highlighted in the data from PMMA, shown in the lower panel of Figure 7. The plot includes data from previous experiments on crosslinked PMMA (black points) drawn from reference [31]. The data from both linear and crosslinked material can be easily fit with a single line, and shows no substantial deviations within the range of temperatures and aging times observed. This shows that the presence or absence of crosslinking (up to a crosslinking density of 1.5%) affects the relaxation times obtained from either technique in an identical fashion.

Considering the power law slopes of the data shown in Figure 7, we present two observations. First, different reasonable efforts to analyze our data will result in somewhat different values for these slopes. For example, in fitting our data to the KWW function, we assumed that the β parameter was constant for both the optical and mechanical measurements. We presented arguments in favor of this procedure above but it certainly is the case that the limited time window for observing the optical and mechanical decay functions covers only a small portion of the distribution of relaxation times implied by these KWW β values; thus one must acknowledge the potential for systematic error. In order to assess the impact of our fitting procedure on the slopes in Figure 7, for a subset of the data, we have constructed an alternate version of this figure by shifting the experimental data and plotting the shift factors instead of KWW τ values. The resulting graphs (included in the supplemental information) also show a strong correlation between the optical and mechanical relaxation functions. For this procedure based upon data shifting, the power law slopes are closer to unity than shown in Figure 7. Thus while our major conclusion of a strong correlation between segmental relaxation processes observed optically and mechanically is supported, the precise values of the power law slopes are uncertain. Secondly, we do not consider a power law slope other than unity is necessarily a result of error, or an indication that

one of these two methods is better than the other. Rather, it is reasonable that the two measurement techniques are sensitive to slightly different aspects of the segmental relaxation process. It is not uncommon for different measurement techniques to report slightly different temperature dependences for relaxation processes.⁵³⁻⁵⁵ Simon et. al., reported that the time for the enthalpy and density to reach equilibrium following a temperature jump can differ for glassy materials, including selenium, polystyrene and poly(ether imide).⁵⁶ We also note that the t values reported in Figure 7 are averages that reflect an underlying distribution of relaxation times spanning 2-4 decades. In this light, a relative shift of 0.2 or 0.3 decades between the two measurements (as seen in Figure 7) over a span of 3 decades in the measured relaxation times is a small effect.

The vertical offset between the data and the reference curves in Figure 7 indicates that in both PLA and PMMA glasses the probe molecules reorient somewhat more slowly than the stress relaxes. In PLA, the ratio between probe reorientation times and stress relaxation times is a factor of ~10, while it is ~3 in PMMA. Such offsets, with probe reorientation measurements giving longer relaxation times than other techniques, have been previously reported.^{30,57} It is often observed that, for a given system, larger probes have longer relaxation times.^{30,57} Thus we attribute the offsets in Figure 7 to indicate that the probe molecule is sensitive to dynamics on a slightly larger length scale than is stress relaxation, and that this effect is more pronounced for PLA than for PMMA.

Probe reorientation measurements collected under active deformation in the post-yield flow regime from PLA and PMMA are also consistent with the vertical offsets in the data shown in Figure 7. It has been observed that for the same probe at the same strain rate and similar temperatures relative to T_g, probe reorientation in PLA is roughly 3 times slower than in PMMA.⁵⁸ Under these conditions, the segmental relaxation times are expected to be approximately equal, and thus this result from the non-linear deformation experiments is consistent with the larger offset observed for PLA in Figure 7.

A further consideration in comparing the vertical offsets in Figure 7 is the use of the 1/e decay time for the optical and mechanical relaxation functions. For processes that are nonexponential, there is no unambiguous choice for comparing relaxation times. If we had utilized the correlation time τ_c (the integral of the correlation function) instead the 1/e decay time, the ratio of optical to mechanical relaxation times for PLA would be about 6 rather than about 10 (as shown in Figure 7A). Similarly for PMMA, the ratio of optical to mechanical relaxation times would be about 5 rather than about 3.

Aging Rates

The rate at which aging proceeds can be quantified by the aging exponent, μ , where

$$\mu = \frac{d \log \tau}{d \log t_a} \tag{2}$$

in a definition analogous to that employed by Struik. ¹⁹ Thus the slopes of linear fits to the data, as shown in Figures 3 and 6, give values for μ . These values are compiled in Figure 8. In this figure, μ values obtained from experiments on PLA under high humidity conditions have been plotted using a T_g value that is 3 K lower, as discussed in the results section.

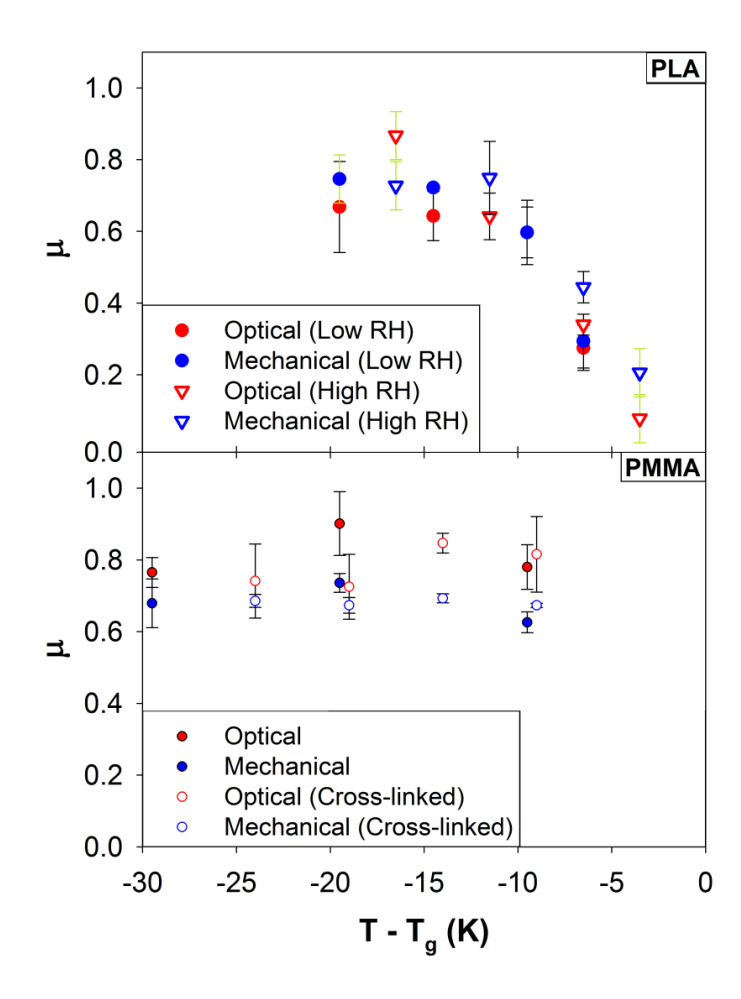


Figure 8. Aging exponents (μ) vs temperature. Red points indicate data from probe reorientation measurements. Blue points indicate data from stress relaxation measurements. Black error bars indicate 1 standard deviation. Upper (PLA): Solid points indicate data collected under low humidity conditions. Open points indicate data collected under high humidity conditions, and have been shifted to the right by 3 K to account for the effect of humidity upon Tg (see text). Green error bars are associated with data points drawn from a single experiment, and are sized to be representative of the error observed in experiments under other conditions. Lower (PMMA): Solid points indicate data from this work on uncrosslinked PMMA. Open points indicate data collected from crosslinked PMMA, drawn from Ref [31].

The PLA results shown in the upper panel of Figure 8 provide a view of polymer glass aging that is easily interpreted. μ values increase from low values near T_g to a value near 1 at a temperature a few tens of Kelvin lower, as the thermodynamic driving force to reach the equilibrium state increases. The

observation that data from high and low humidity reasonably follows a single curve supports the view that the increased water content in the samples under high humidity acts to shift T_g by ~3 K.

In the lower panel of Figure 8, PMMA data from uncrosslinked samples is shown alongside previously collected data from crosslinked PMMA samples.³¹ No significant temperature dependence in the aging rate is observed from either sample, with results indicating an approximately constant value of ~0.7 for both crosslinked and uncrosslinked material. Struik indicates that aging rates in PMMA (determined from creep experiments) are still increasing at the high end of the temperature window presented here, and reach a value of ~1 within the range of temperatures investigated. ¹⁹ In a previous publication,³¹ we posited that the discrepancy between our observations and Struik's were due to the crosslinked nature of our samples.⁵⁹ The observations presented here indicate that the presence or absence of a small degree of crosslinking in PMMA samples does not significantly influence the aging behavior within this temperature window, and so there must be a different reason (as yet unidentified) for the difference in behavior reported by Struik. We note that the temperature range examined for PMMA is not identical to that examined for PLA. This is due to the difficulty of optically measuring relaxation times of less than ~100 seconds, a condition that occurs at different temperatures (relative to T_g) for the two materials. In PLA, μ begins to become strongly temperature dependent at temperatures near to T_g-10, which is the highest relative temperature evaluated for PMMA. We expect that PMMA would age at slower rates if tested at higher temperatures than were utilized here. Previous volumetric measurements of PMMA have observed unusual aging behavior at very low temperatures, including the presence of a peak in the aging rate about 110 K below Tg. 60 These features are generally attributed to the presence of a secondary relaxation processes.

Secondary relaxations

One important distinction between the polymer systems investigated here is that PMMA is known to have a (faster) secondary relaxation process that overlaps with the α process near T_g , $^{45-46}$ while no such secondary relaxation process is active in PLA within the temperature range employed. 44 , 47 , 61 In comparing results between materials with and without an active secondary relaxation process, we interpret Figure 7 to mean that secondary relaxations do not affect the strong correlation between stress relaxation time and the probe reorientation time. The simplest explanation is that the secondary relaxation in PMMA has little impact on either observable. Thus the probe reorientation time is a good reporter of the segmental dynamics even in a system with prominent secondary relaxation processes.

Data collected from stress relaxation experiments on the PMMA sample exhibits some minor features at short times that may be associated with the presence of a secondary relaxation overlapping the α process. The KWW fit to the master curve of all stress relaxation data (Figures 2 and 5) is better in PLA than in PMMA. The deviation between the data and the KWW function for PMMA only extends over the first ~10 seconds of a given measurement, which are collected over a span of 3-50 minutes, and is only observable in experiments performed at the lowest temperature, 375 K. A similar deviation of the KWW fit from the stress relaxation data was reported for crosslinked PMMA.³¹ This early decay may be compatible with the end of a secondary relaxation process. The effects of this initial misfit on the relaxation times obtained from fits to the entire curve are negligible.

Conclusions

Here we have measured probe reorientation times and stress relaxation times in two different polymer glasses. The measured relaxation times depend primarily upon the temperature and the aging time, but other parameters, such as the relative humidity in experiments with PLA, can influence the dynamics. For both PLA and PMMA glasses, the probe reorientation times are strongly correlated with stress relaxation times over a range of aging times and aging temperatures. By comparing these results

with previous work on crosslinked PMMA,³¹ we conclude that the strong correlation between probe reorientation and stress relaxation measurements is maintained despite differences in polymer structure. While the presence of plasticizers, crosslinking, and secondary relaxations have an important influence on polymer dynamics, in these experiments they do not influence the correlation between relaxation times obtained from probe reorientation and stress relaxation.

The broader context for this work is our interest in measuring segmental dynamics during the nonlinear deformation of polymer glasses. The present results are an important confirmation of the reliability of the probe reorientation technique for measuring glassy dynamics in the linear response regime. The current work is consistent with the view that probe reorientation provides a viable experimental avenue to investigate changes in mobility in glassy polymers, including during non-linear deformation, and can provide a quantitative measurement of segmental relaxation times.

Acknowledgements

We thank the National Science Foundation (DMR-1708248) for support of this work. The authors thank Brock Lynde for his assistance with NMR experiments. TB gratefully acknowledges helpful discussions with Selina Ortiz Piccard in the course of this work.

Supporting Information

KWW β values determined from unconstrained fits to both probe reorientation data and stress relaxation data, and an alternate scheme for comparison of probe reorientation and stress relaxation measurements.

References

1. Wang, S.-Q.; Cheng, S.; Lin, P.; Li, X., A phenomenological molecular model for yielding and brittle-ductile transition of polymer glasses. *J. Chem. Phys.* **2014**, *141* (9).

- 2. Li, X.; Wang, S.-Q., Mapping Brittle and Ductile Behaviors of Polymeric Glasses under Large Extension. *ACS Macro Lett.* **2015**, *4* (10), 1110-1113.
- 3. Kierkels, J. T. A.; Dona, C. L.; Tervoort, T. A.; Govaert, L. E., Kinetics of re-embrittlement of (anti)plasticized glassy polymers after mechanical rejuvenation. *J. Polym. Sci., Part B: Polym. Phys.* **2008**, *46* (2), 134-147.
- 4. Lee, H.-N.; Ediger, M. D., Mechanical Rejuvenation in Poly(methyl methacrylate) Glasses? Molecular Mobility after Deformation. *Macromolecules* **2010**, *43* (13), 5863-5873.
- 5. Klompen, E. T. J.; Engels, T. A. P.; Govaert, L. E.; Meijer, H. E. H., Modeling of the Postyield Response of Glassy Polymers: Influence of Thermomechanical History. *Macromolecules* **2005**, *38* (16), 6997-7008.
- 6. McKenna, G. B., Mechanical rejuvenation in polymer glasses: fact or fallacy? *J Phys-Condens Mat* **2003**, *15* (11), S737-S763.
- 7. Eyring, H., Viscosity, Plasticity, and Diffusion as Examples of Absolute Reaction Rates. *J. Chem. Phys.* **1936**, *4* (4), 283-291.
- 8. Hudzinskyy, D.; Michels, M. A. J.; Lyulin, A. V., Rejuvenation, Aging, and Confinement Effects in Atactic-Polystyrene Films Subjected to Oscillatory Shear. *Macromol. Theory Simul.* **2013**, *22* (1), 71-84.
- 9. Riggleman, R. A.; Lee, H.-N.; Ediger, M. D.; de Pablo, J. J., Heterogeneous dynamics during deformation of a polymer glass. *Soft Matter* **2010**, *6* (2), 287-291.
- 10. Rottler, J., Relaxation times in deformed polymer glasses: A comparison between molecular simulations and two theories. *J. Chem. Phys.* **2016**, *145* (6).
- 11. Chen, K.; Schweizer, K. S., Theory of Yielding, Strain Softening, and Steady Plastic Flow in Polymer Glasses under Constant Strain Rate Deformation. *Macromolecules* **2011**, *44* (10), 3988-4000.
- 12. Fielding, S. M.; Larson, R. G.; Cates, M. E., Simple model for the deformation-induced relaxation of glassy polymers. *Phys. Rev. Lett.* **2012**, *108* (4), 048301.
- 13. Long, D. R.; Conca, L.; Sotta, P., Dynamics in glassy polymers: The Eyring model revisited. *Physical Review Materials* **2018**, *2* (10).
- 14. Medvedev, G. A.; Caruthers, J. M., Development of a stochastic constitutive model for prediction of postyield softening in glassy polymers. *J. Rheol.* **2013,** *57* (3), 949-1002.
- 15. Govaert, L. E.; Timmermans, P. H. M.; Brekelmans, W. A. M., The Influence of Intrinsic Strain Softening on Strain Localization in Polycarbonate Modeling. *J. Eng. Mater. Technol.* **2000**, *122*, 177-185.
- 16. Tervoort, T. A.; Klompen, E. T. J.; Govaert, L. E., A multi-mode approach to finite, three-dimensional, nonlinear viscoelastic behavior of polymer glasses. *J. Rheol.* **1996**, *40* (5), 779-797.
- 17. Kalfus, J.; Detwiler, A.; Lesser, A. J., Probing Segmental Dynamics of Polymer Glasses during Tensile Deformation with Dielectric Spectroscopy. *Macromolecules* **2012**, *45* (11), 4839-4847.
- Pérez-Aparicio, R.; Cottinet, D.; Crauste-Thibierge, C.; Vanel, L.; Sotta, P.; Delannoy, J.-Y.; Long,
 D. R.; Ciliberto, S., Dielectric Spectroscopy of a Stretched Polymer Glass: Heterogeneous
 Dynamics and Plasticity. *Macromolecules* 2016, 49 (10), 3889-3898.
- 19. Struik, L. C. E., *Physical Aging in Amorphous Polymers and Other Materials*. Elsevier Scientific: New York, 1977.
- 20. McKenna, G. B.; Zapas, L. J., Superposition of small strains on large deformations as a probe of nonlinear response in polymers. *Polym. Eng. Sci.* **1986**, *26* (11), 725-729.
- 21. Bending, B.; Christison, K.; Ricci, J.; Ediger, M. D., Measurement of Segmental Mobility during Constant Strain Rate Deformation of a Poly(methyl methacrylate) Glass. *Macromolecules* **2014**, *47* (2), 800-806.

- Lee, H. N.; Paeng, K.; Swallen, S. F.; Ediger, M. D., Dye reorientation as a probe of stress-induced mobility in polymer glasses. *J. Chem. Phys.* **2008**, *128* (13), 134902.
- 23. Lee, H. N.; Paeng, K.; Swallen, S. F.; Ediger, M. D., Direct measurement of molecular mobility in actively deformed polymer glasses. *Science* **2009**, *323* (5911), 231-4.
- 24. Chen, K.; Schweizer, K. S., Theory of aging, rejuvenation, and the nonequilibrium steady state in deformed polymer glasses. *Phys. Rev. E: Stat., Nonlinear, Soft Matter Phys.* **2010,** *82* (4 Pt 1), 041804.
- 25. Dequidt, A.; Conca, L.; Delannoy, J.-Y.; Sotta, P.; Lequeux, F.; Long, D. R., Heterogeneous Dynamics and Polymer Plasticity. *Macromolecules* **2016**, *49* (23), 9148-9162.
- 26. Medvedev, G. A.; Caruthers, J. M., Stochastic model prediction of nonlinear creep in glassy polymers. *Polymer* **2015**, *74*, 235-253.
- 27. Zou, W.; Larson, R. G., A hybrid Brownian dynamics/constitutive model for yielding, aging, and rejuvenation in deforming polymeric glasses. *Soft Matter* **2016**, *12* (32), 6757-70.
- 28. Conca, L.; Dequidt, A.; Sotta, P.; Long, D. R., Acceleration and Homogenization of the Dynamics during Plastic Deformation. *Macromolecules* **2017**, *50* (23), 9456-9472.
- 29. Dhinojwala, A.; Wong, G. K.; Torkelson, J. M., Rotational reorientation dynamics of disperse red 1 in polystyrene: α -relaxation dynamics probed by second harmonic generation and dielectric relaxation. *J. Chem. Phys.* **1994**, *100* (8), 6046-6054.
- 30. Inoue, T.; Cicerone, M. T.; Ediger, M. D., Molecular Motions and Viscoelasticity of Amorphous Polymers near Tg. *Macromolecules* **1995**, *28* (9), 3425-3433.
- 31. Ricci, J.; Bennin, T.; Ediger, M. D., Direct Comparison of Probe Reorientation and Linear Mechanical Measurements of Segmental Dynamics in Glassy Poly(methyl methacrylate). *Macromolecules* **2018**, *51* (19), 7785-7793.
- 32. Arruda, E. M.; Boyce, M. C.; Jayachandran, R., Effects of Strain-Rate, Temperature and Thermomechanical Coupling on the Finite Strain Deformation of Glassy-Polymers. *Mech. Mater.* **1995**, *19* (2-3), 193-212.
- 33. Bauwens-Crowet, C., The compression yield behaviour of polymethyl methacrylate over a wide range of temperatures and strain-rates. *J. Mat. Sci.* **1973**, *8* (7), 968-979.
- 34. Bending, B.; Ediger, M. D., Comparison of mechanical and molecular measures of mobility during constant strain rate deformation of a PMMA glass. *J. Polym. Sci., Part B: Polym. Phys.* **2016**, *54* (19), 1957-1967.
- 35. Hebert, K.; Bending, B.; Ricci, J.; Ediger, M. D., Effect of Temperature on Postyield Segmental Dynamics of Poly(methyl methacrylate) Glasses: Thermally Activated Transitions Are Important. *Macromolecules* **2015**, *48* (18), 6736-6744.
- 36. Kim, J. W.; Medvedev, G. A.; Caruthers, J. M., The response of a glassy polymer in a loading/unloading deformation: The stress memory experiment. *Polymer* **2013**, *54* (21), 5993-6002.
- 37. Lee, H.-N.; Paeng, K.; Swallen, S. F.; Ediger, M. D.; Stamm, R. A.; Medvedev, G. A.; Caruthers, J. M., Molecular mobility of poly(methyl methacrylate) glass during uniaxial tensile creep deformation. *J. Polym. Sci., Part B: Polym. Phys.* **2009**, *47* (17), 1713-1727.
- 38. Sun, H.; Liu, G.; Ntetsikas, K.; Avgeropoulos, A.; Wang, S.-Q., Rheology of Entangled Polymers Not Far above Glass Transition Temperature: Transient Elasticity and Intersegmental Viscous Stress. *Macromolecules* **2014**, *47* (16), 5839-5850.
- 39. Garlotta, D., A literature review of poly(lactic acid). J Polym Environ 2001, 9 (2), 63-84.
- 40. Drumright, R. E.; Gruber, P. R.; Henton, D. E., Polylactic acid technology. *Advanced Materials* **2000**, *12* (23), 1841-1846.

- 41. Danhier, F.; Ansorena, E.; Silva, J. M.; Coco, R.; Le Breton, A.; Preat, V., PLGA-based nanoparticles: an overview of biomedical applications. *J Control Release* **2012**, *161* (2), 505-22.
- 42. Madhavan Nampoothiri, K.; Nair, N. R.; John, R. P., An overview of the recent developments in polylactide (PLA) research. *Bioresour Technol* **2010**, *101* (22), 8493-501.
- 43. Huang, T.; Miura, M.; Nobukawa, S.; Yamaguchi, M., Chain Packing and Its Anomalous Effect on Mechanical Toughness for Poly(lactic acid). *Biomacromolecules* **2015**, *16* (5), 1660-6.
- 44. Mijovic, J.; Sy, J. W., Molecular dynamics during crystallization of poly(L-lactic acid) as studied by broad-band dielectric relaxation spectroscopy. *Macromolecules* **2002**, *35* (16), 6370-6376.
- 45. Bergman, R.; Alvarez, F.; Alegria, A.; Colmenero, J., Dielectric relaxation in PMMA revisited. *J. Non-Cryst. Solids* **1998**, *235*, 580-583.
- 46. Bergman, R.; Alvarez, F.; Alegría, A.; Colmenero, J., The merging of the dielectric α and β relaxations in poly-(methyl methacrylate). *J. Chem. Phys.* **1998**, *109* (17), 7546-7555.
- 47. Mierzwa, M.; Floudas, G.; Dorgan, J.; Knauss, D.; Wegner, J., Local and global dynamics of polylactides. A dielectric spectroscopy study. *J. Non-Cryst. Solids* **2002**, *307*, 296-303.
- 48. Sharp, J. S.; Forrest, J. A.; Jones, R. A. L., Swelling of Poly(DL-lactide) and polylactide-co-glycolide in humid environments. *Macromolecules* **2001**, *34* (25), 8752-8760.
- Zell, M. T.; Padden, B. E.; Paterick, A. J.; Thakur, K. A. M.; Kean, R. T.; Hillmyer, M. A.; Munson, E. J., Unambiguous Determination of the 13C and 1H NMR Stereosequence Assignments of Polylactide Using High-Resolution Solution NMR Spectroscopy. *Macromolecules* 2002, 35 (20), 7700-7707.
- 50. O Connell, P. A.; McKenna, G. B., Large deformation response of polycarbonate: Time-temperature, time-aging time, and time-strain superposition. *Polym. Eng. Sci.* **1997,** *37* (9), 1485-1495.
- 51. Buck, A. L., New Equations for Computing Vapor-Pressure and Enhancement Factor. *J Appl Meteorol* **1981**, *20* (12), 1527-1532.
- 52. Shi, X.; Mandanici, A.; McKenna, G. B., Shear stress relaxation and physical aging study on simple glass-forming materials. *J. Chem. Phys.* **2005**, *123* (17), 174507.
- 53. Inoue, T.; Okamoto, H.; Osaki, K., Birefringence of amorphous polymers. 1. Dynamic measurement on polystyrene. *Macromolecules* **1991**, *24* (20), 5670-5675.
- 54. Plazek, D. J., Temperature Dependence of the Viscoelastic Behavior of Polystyrene. *J. Phys. Chem.* **1965**, *69* (10), 3480-3487.
- 55. Thurau, C. T.; Ediger, M. D., Change in the temperature dependence of segmental dynamics in deeply supercooled polycarbonate. *J. Chem. Phys.* **2003**, *118* (4), 1996-2004.
- 56. Badrinarayanan, P.; Simon, S. L., Origin of the divergence of the timescales for volume and enthalpy recovery. *Polymer* **2007**, *48* (6), 1464-1470.
- 57. Paeng, K.; Kaufman, L. J., Single Molecule Experiments Reveal the Dynamic Heterogeneity and Exchange Time Scales of Polystyrene near the Glass Transition. *Macromolecules* **2016**, *49* (7), 2876-2885.
- 58. Bennin, T.; Ricci, J.; Ediger, M. D., Enhanced Segmental Dynamics of Poly(lactic acid) Glasses during Constant Strain Rate Deformation. *Macromolecules* **2019**, *52* (17), 6428-6437.
- 59. Jin, K.; Li, L.; Torkelson, J. M., Bulk physical aging behavior of cross-linked polystyrene compared to its linear precursor: Effects of cross-linking and aging temperature. *Polymer* **2017**, *115*, 197-203.
- 60. Greiner, R.; Schwarzl, F. R., Thermal Contraction and Volume Relaxation of Amorphous Polymers. *Rheologica Acta* **1984,** *23* (4), 378-395.

61. van Breemen, L. C. A.; Engels, T. A. P.; Klompen, E. T. J.; Senden, D. J. A.; Govaert, L. E., Rate- and temperature-dependent strain softening in solid polymers. *J. Polym. Sci., Part B: Polym. Phys.* **2012**, *50* (24), 1757-1771.